RESEARCH ARTICLE

Chromone–lipoic acid conjugate: Neuroprotective agent having acceptable butyrylcholinesterase inhibition, antioxidant and copper-chelation activities

Leili Jalili-Baleh[1] · Hamid Nadri[2] · Hamid Forootanfar[3] · Tuba Tüylü Küçükkılınç[4] · Beyza Ayazgök[4] · Mohammad Sharifzadeh[5] · Mahban Rahimifard[6] · Maryam Baeeri[6] · Mohammad Abdollahi[6] · Alireza Foroumadi[1] · Mehdi Khoobi[1]

Abstract

Purpose Alzheimer's disease (AD) is a multifaceted neurodegenerative disease. To target simultaneously multiple pathological processes involved in AD, natural-origin compounds with unique characteristics are promising scaffolds to develop novel multi-target compounds in the treatment of different neurodegenerative disease, especially AD. In this study, novel chromone-lipoic acid hybrids were prepared to find a new multifunctional lead structure for the treatment of AD.

Methods Chromone-lipoic acid hybrids were prepared through click reaction and their neuroprotection and anticholinesterase activity were fully evaluated. The anti-amyloid aggregation, antioxidant and metal-chelation activities of the best compound were also investigated by standard methods to find a new multi-functional agent against AD.

Results The primary biological screening demonstrated that all compounds had significant neuroprotection activity against H2O2-induced cell damage in PC12 cells. Compound 19 as the most potent butyrylcholinesterase (BuChE) inhibitor (IC50 = 7.55 μM) having significant neuroprotection activity as level as reference drug was selected for further biological evaluations. Docking and kinetic studies revealed non-competitive mixed-type inhibition of BuChE by compound 19. It could significantly reduce formation of the intracellular reactive oxygen species (ROS) and showed excellent reducing power (85.57 mM Fe+2), comparable with quercetin and lipoic acid. It could also moderately inhibit Aβ aggregation and selectively chelate with copper ions in 2:1 M ratio.

Conclusion Compound 19 could be considered as a hopeful multifunctional agent for the further development gainst AD owing to the acceptable neuroprotective and anti-BuChE activity, moderate anti-Aβ aggregation activity, outstanding antioxidant activity as well as selective copper chelation ability.

✉ Mehdi Khoobi
    Mehdi.khoobi@gmail.com

1   Biomaterials Group, Pharmaceutical Research Center, The Institute of Pharmaceutical Sciences (TIPS), Tehran University of Medical Sciences, Tehran 1417614411, Iran

2   Faculty of Pharmacy and Pharmaceutical Sciences Research Center, Shahid Sadoughi University of Medical Sciences, Yazd, Iran

3   Department of Pharmaceutical Biotechnology, Faculty of Pharmacy, Kerman University of Medical Sciences, Kerman, Iran

4   Faculty of Pharmacy, Department of Biochemistry, Hacettepe University, Ankara, Turkey

5   Department of Pharmacology and Toxicology, Faculty of Pharmacy, Toxicology and poisoning Research Centre, Tehran University of Medical Sciences, Tehran, Iran

6   Toxicology and Diseases Group, Pharmaceutical Sciences Research Center (PSRC), The Institute of Pharmaceutical Sciences (TIPS), Tehran University of Medical Sciences (TUMS), Tehran, Iran

 Springer

Introduction

Alzheimer's disease (AD), a multifaceted and irreversible neurodegenerative disease, is the major cause of dementia, and one of the biggest challenges of current pharmaceutical research [1]. During the past decades, despite substantial efforts to discover the pathogenic mechanisms of AD, the exact etiology of this disease is still complex in nature. The pathological factors playing remarkable role in development of AD are deficiency of brain cholinergic neurotransmitters level, accumulation of senile plaques particularly as extracellular β-amyloid (Aβ) deposits, hyperphosphorylated τ-protein aggregation [2], dyshomeostasis of biometals, oxidative stress, and neuroinflammation [3].

Notwithstanding all attempts performed to find innovative solution to control the hallmarks of the disease like gen and stem cell therapy, but these kind of therapies are still a prospective method for AD treatment and there are still many unsolved problems before they can be used in clinical applications [4, 5]. The currently available therapeutic method is mostly based on the increasing cholinergic neurotransmission, through acetylcholinesterase inhibitors (AChEI). Like AChE, butyrylcholinesterase (BuChE) as a coregulator of the ACh degradation, is an important enzyme involved in the neurotransmission [6]. The role of BuChE in AD pathology is unknown, but in vivo studies revealed that BuChE associated with Aβ plaques has key role in AD plaque maturation [7, 8]. To complete the symptomatic approaches, it is necessary to target simultaneously multiple pathological processes involved in AD [9, 10]. Currently, multi-target directed ligand (MTDL) strategy has been completely accepted as the main strategy for the drug design and discovery in AD, which is based on combination of appropriate pharmacophoric groups in one-molecule providing effective pharmacological responses for various potential receptors or enzymatic targets [11]. In recent years, many potential multifunctional agents have been designed based on MTDLs strategy against AD [12–16].

Moreover, quite an amount of natural-origin products is being used either as marketed pharmaceuticals or as bioactive molecular fragments in the development of hybrid drugs to combat the above-referred major risk factors involved in the pathogenesis of AD [17]. Chromones are ubiquitously found in plants and are known as the phytochemicals with a benzo-γ-pyrone structure, which possess a multiple range of pharmacological effects [18]. Recent studies revealed that chromone-based compounds were effective against dementia through free radicals scavenging and metal ions chelating [19–22]. Chromones have also showed anticholinesterase [23, 24], neuroprotective [25, 26], anti-inflammatory properties [27], and could effectively disrupt amyloid-β aggregation [28, 29]. Fernandez-Bachiller and co-workers introduced tacrine-chromone hybrids having improved ChE inhibitory as well as antioxidant activates compared to tacrine [30].

Lipoic acid (LA), as a naturally occurring antioxidant in animals, humans, and plants acts as an essential cofactor in many biochemical pathways [31]. Diverse range of pharmacological properties has been reported about this organosulfur. It can control the pathogenesis or progression of AD by increasing the level of acetylcholine as well as decreasing oxidative stress, inflammation, and Aβ plaque formation [32–34]. Lipocrine as a hybrid of LA and tacrine introduced by Rosini as an effective drug candidate against AD due to its multiple biological properties, such as AChE and BChE inhibition activity, inhibition of AChE-induced Aβ aggregation, and cell protectetion against ROS [35]. G. Nesi et al. combined rivastigmine with LA and chromone. They found that the combination led to the addition of anti-oxidants and anti-amyloid aggregating properties of LA and chromone scaffolds to the anticholinesterase activity of rivastigmine as the currently used drugs, and resulted to the formation of multifunctional compound to treat AD [28].

Based on the above findings, chromone scaffold is an important pharmacophore having great role in ChEs inhibition with antioxidant and metal chelation activities. LA is also the promising lead structure improving BuChE inhibition activity, neuroprotection potency, anti-amyloid aggregation, antioxidant and metal chelation activities (Fig. 1). These unique characteristics of chromone and LA have made them as promising scaffolds to develop novel multi-target compounds having improved therapeutic efficacy in the treatment of different neurodegenerative disorders, especially AD [36–42]. Considering the beneficial biological effects of chromone and LA scaffolds and the efficacy of triazole nucleus as an attractive pharmacophore to connecting various therapeutically active agents [43–45], in this work, we encouraged to conjugate these valuabe pharmacophores to each other and evaluate their efficacy against various targets. Two series of chromone derivatives conjugated with LA were synthesized via click reaction (Fig. 1, compounds **9–17** and **18–20**) and the neuroprotective activity and ChEs inhibition activity of all the compounds were evaluated. The antioxidant, metal chelation and anti-amyloid activities of the selected compound was also evaluated. To the best of our knowledge, this is the first work reporting the synthesis of chromone-LA hybrids and their biological activities against AD.

Experimental

Chemistry

Chemicals and solvents were obtained from commercial companies. Kofler hot stage apparatus was applied to determine melting points. The KBr disk method was used for FTIR

Fig. 1 Designed strategy for the preparation of the new chromone-LA hybrids

Designed compounds **9-20**
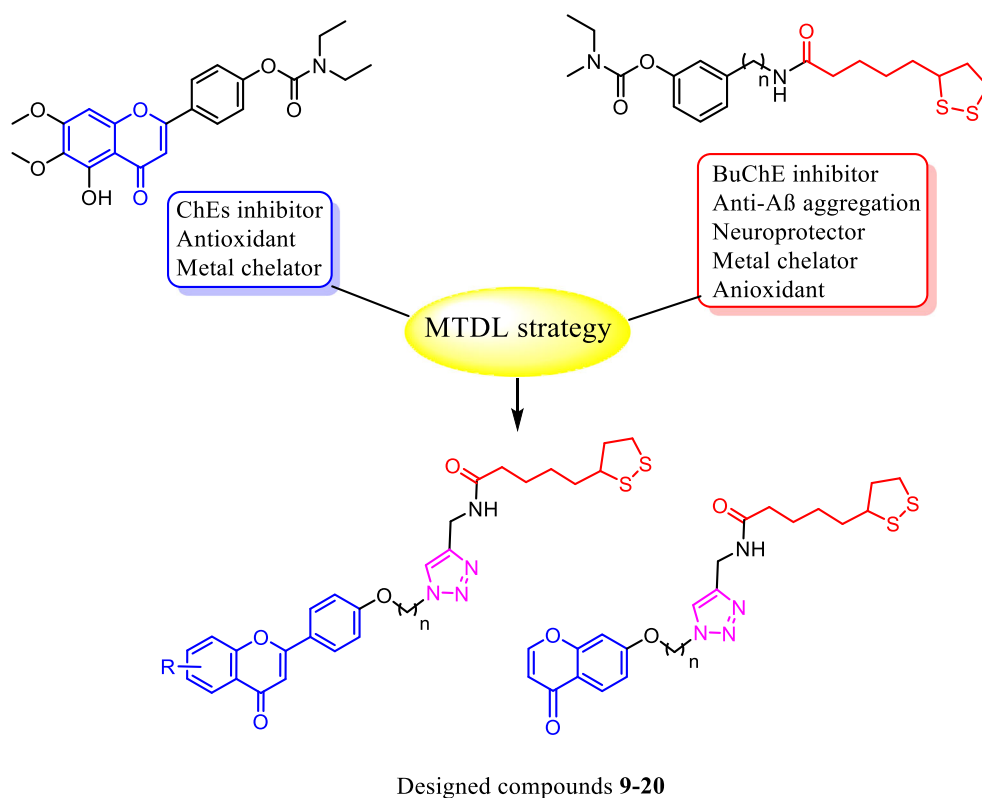
analysis taken by Nicolet Magna FTIR-550 spectrometer. Brucker FT-500 was used for ^{1}H and ^{13}C NMR spectra. Elemental analysis of the compounds was performed on CHN-Rapid Heraeus Elemental Analyzer. The UV-Vis absorption spectra were recorded on a double beam GBC Cintra 101.

General method for the preparation of compounds 4a-d

2′-Hydroxyacetophenone derivative (**1a-d**, 1 equiv) was mixed with 4-methoxybenzaldehyde (**2**, 1 equiv) in the presence of pyrrolidine (0.5 equiv) and iodine (10 mol%) as catalyst in DMSO as solvent under reflux for 2 h. After finishing the reaction monitored by thin-layer chromatography (TLC), the reaction was worked up by ethylacetate and water. The organic part was wahsed with water, saturated sodium thiosulfate solution, brine, and finally dried by anhydrous sodium sulfate. The organic solvent was removed by rotary evaporator and the purified compound was obtained by column chromatography [46]. Then, the corresponding methoxyflavone (**3a-d**, 1 mmol) was dissolved in dry CH_2Cl_2 (15 mL) and temperature of the reaction decreased to −60 °C and BBr$_3$ (3 mmol) was next added dropwise to the solution. The reaction was kept to be stirred at ambient temperature for 24 h until completion of the reaction. After that, ice water (50 mL) was added to the reaction and the product was extracted with ethylacetate (2 × 30 mL). The organic layer was then mixed

with water, brine, and dried by anhydrous Na$_2$SO$_4$. The solvent was evaporated under vacuum and the product was used with no more purification [47].

General method for the preparation of 7-Hydroxy-4H-l-benzopyran-4-one (compound 5)

2,4-Dihydroxyacetophenone (1 mmol) in triethyl orthoformate (1 mL) was stirred, and 70% perchloric acid (0.1 mL) was next added dropwise. A dark solution was formed and the temperature of the mixture increased slightly. Anhydrous ethyl ether (3 mL) was next added to form a brown precipitate. The product was filtered, dissolved in hot water (2 mL), and refluxed for 5 min. The mixture was then cooled to ambient temperature overnight. A dark product was filtered and recrystallized from water/ethanol [48].

General method for the synthesis of bromoalkoxy intermediates 6a-i, and 8a-c

A mixture of hydroxylated chromone derivative (1 mmol), anhydrous K$_2$CO$_3$ (2 mmol) and appropriate dibromoalkane (10 mmol) was refluxed in acetone (5 mL). The precipitate was filtered off after 4 h and washed with acetone. Then, the acetone was removed under vacuum and the product was treated with petroleum ether to precipitate the pure product [49].

General method for the preparation of 1,2-dithiolane-3-pentanoic acid-*N*-propargylamide (compound 7)

LA (1 mmol), DMAP (1.2 mmol) and N-Ethyl-N′-(3-dimethylaminopropyl)carbodiimide hydrochloride (EDCI, 1.2 mmol) was mixed in anhydrous CH_2Cl_2 (10 mL) at 0 °C. Then, propargylamine (1.2 mmol) in 2 mL dry CH_2Cl_2 was added dropwise and the reaction was performed at ambient temperature for 12 h. When the reaction was completed, the solvent was removed under vacuum and the crude product was obtained by column chromatography eluted by petroleum ether/ethyl acetate/(2:1) [50].

General method for the preparation of chromone–LA conjugates 9–20

A solution of the corresponding intermediate (**6a-i,** and **8a-c**, 1 mmol), sodium azide (1 mmol), triethylamine (1 mmol) in *t*-BuOH (4 mL) and H_2O (4 mL) was stirred at 70 °C for 0.5 h. After that, compound **7** (1 mmol), $CuSO_4.5H_2O$ (0.2 mmol), and sodium ascorbate (0.2 mmol) were added to the reaction and it was stirred for 12 h. When the reaction was completed, water was added to the mixture and the reaction was stirred for next 0.5 h. Then, the mixture was filtered off and the product was purified by flash chromatography on silica gel eluted with petroleum ether / ethyl acetate (1:1) to give pure products **9–20** with 80–99% yields [51].

Characterization and structural determination of the synthesized products

5-(1,2-dithiolan-3-yl)-N-((1-(3-(4-(4-oxo-4H-chromen-2-yl)phenoxy)propyl)-1H-1,2,3-triazol-4-yl)methyl)pentanamide (9) Off-white solid; mp 130–132 °C; IR (KBr, cm^{-1}) ν_{max}: 3300 (NH), 2930 (C-H), 1621 (C=O). ^1H NMR (DMSO-d_6, 500 MHz) δ: 8.23 (t, 1H, J = 5.5 Hz, NH), 8.04 (d, 2H, J = 9.0 Hz, phenoxy), 8.04 (d, 1H, J = 7.5 Hz, H_5), 7.93 (s, 1H, triazole), 7.80 (t, 1H, J = 7.5 Hz, H_7), 7.76 (d, 1H, J = 7.5 Hz, H_8), 7.49 (t, 1H, J = 7.5 Hz, H_6), 7.10 (d, 2H, J = 9.0 Hz, phenoxy), 6.93 (s, 1H, H_3), 4.53 (t, 2H, J = 7.0 Hz, CH$_2$-N), 4.28 (d, 2H, J = 5.5 Hz, CH$_2$-NH), 4.09 (t, 2H, J = 6.5 Hz, CH$_2$-O), 3.57 (quintet, 1H, J = 6.0 Hz, CH-S), 3.17-3.08 (m, 2H, CH$_2$-S), 2.38 (sextet, 1H, J = 6.7 Hz, S-CH$_2$-C$\underline{H}_2$), 2.29 (quintet, 2H, aliphatic chain), 2.09 (t, 2H, J = 7.5 Hz, CH$_2$-CO), 1.83 (sextet, 1H, J = 7.0 Hz, S-CH$_2$-C$\underline{H}_2$), 1.65-1.48 (m, 4H, aliphatic chain), 1.33-1.30 (m, 2H, aliphatic chain). ^{13}C NMR (DMSO-d_6, 125 MHz) δ: 176.7, 171.7, 162.5, 161.1, 155.5, 144.9, 133.9, 128.0, 125.2, 124.6, 123.3, 123.2, 122.7, 118.2, 114.9, 105.4, 64.8, 55.9, 46.2, 39.8, 39.7, 37.9, 34.9, 34.0, 33.9, 29.2, 28.1. Anal. Calcd for $C_{29}H_{32}N_4O_4S_2$: C, 61.68; H, 5.71; N, 9.92. Found: C, 61.82; H, 5.43; N, 10.12.

N-((1-(3-(4-(6-bromo-4-oxo-4H-chromen-2-yl)phenoxy)propyl)-1H-1,2,3-triazol-4-yl)methyl)-5-(1,2-dithiolan-3-yl)pentanamide (10) Off-white solid; mp 122–125 °C; IR (KBr, cm^{-1}) ν_{max}: 3306 (NH), 2927 (C-H), 1640 (C=O). ^1H NMR (DMSO-d_6, 500 MHz) δ: 8.25 (t, 1H, J = 5.5 Hz, NH), 8.10 (s, 1H, triazole), 8.08 (d, J = 8.5 Hz, 2H, phenoxy), 7.98 (d, 1H, J = 8.5 Hz, H_7), 7.93 (s, 1H, H_5), 7.78 (d, 1H, J = 8.5 Hz, H_8), 7.10 (d, 2H, J = 8.5 Hz, phenoxy), 7.00 (s, 1H, H_3), 4.53 (t, 2H, J = 6.5 Hz, CH$_2$-N), 4.28 (d, 2H, J = 5.5 Hz, CH$_2$-NH), 4.09 (t, 2H, J = 5.5 Hz, CH$_2$-O), 3.57–3.55 (m, 1H, CH-S), 3.17–3.09 (m, 2H, CH$_2$-S), 2.39–2.34 (m, 1H, S-CH$_2$-C$\underline{H}_2$), 2.31–2.27 (m, 2H, aliphatic chain), 2.08 (t, 2H, J = 7.0 Hz, CH$_2$-CO), 1.84–1.80 (m, 1H, S-CH$_2$-C$\underline{H}_2$), 1.65–1.59 (m, 1H, C$\underline{H}_2$-CH$_2$-CO), 155–1.47 (m, 3H, aliphatic chain), 1.34–1.30 (m, 2H, aliphatic chain). ^{13}C NMR (DMSO-d_6, 125 MHz) δ: 175.8, 171.8, 162.9, 161.3, 154.5, 145.0, 136.9, 128.3, 126.8, 124.8, 123.0, 122.8, 117.7, 115.0, 105.8, 65.2, 56.0, 46.2, 39.1, 34.9, 34.0, 29.3, 28.2, 24.8. Anal. Calcd for $C_{29}H_{31}BrN_4O_4S_2$: C, 54.12; H, 4.86; N, 8.71. Found: C, 54.06; H, 4.55; N, 8.51.

5-(1,2-dithiolan-3-yl)-N-((1-(4-(4-(4-oxo-4H-chromen-2-yl)phenoxy)butyl)-1H-1,2,3-triazol-4-yl)methyl)pentanamide (11) Off-white solid; mp 94–95 °C; IR (KBr, cm^{-1}) ν_{max}: 3298 (NH), 2920 (C-H), 1627 (C=O). ^1H NMR (DMSO-d_6, 500 MHz) δ: 8.30 (t, J = 5.5 Hz, 1H, NH), 8.06 (d, J = 9.0 Hz, 2H, phenoxy), 8.03 (d, J = 7.5 Hz, 1H, H_5), 7.93 (s, 1H, triazole), 7.82 (t, J = 7.5 Hz, 1H, H_7), 7.77 (d, J = 7.5 Hz, 1H, H_8), 7.49 (t, J = 7.5 Hz, 1H, H_6), 7.10 (d, J = 9.0 Hz, 2H, phenoxy), 6.96 (s, 1H, H_3), 4.41 (t, J = 7.0 Hz, 2H, CH$_2$-N), 4.27 (d, J = 5.5 Hz, 2H, CH$_2$-NH), 4.10 (t, J = 6.5 Hz, 2H, CH$_2$-O), 3.57 (quintet, J = 6.0 Hz, 1H, CH-S), 3.16–3.08 (m, 2H, CH$_2$-S), 2.39–2.32 (sextet, 1H, J = 6.7 Hz, S-CH$_2$-C$\underline{H}_2$), 2.08 (t, 2H, J = 7.5 Hz, CH$_2$-CO), 1.96 (quintet, 2H, aliphatic chain), 1.84 (sextet, 1H, J = 7.0 Hz, S-CH$_2$-C$\underline{H}_2$), 1.73–1.70 (m, 2H, aliphatic chain), 1.65–1.60 (m, 1H, C$\underline{H}_2$-CH$_2$-CO), 1.54–1.48 (m, 4H, aliphatic chain), 1.33–1.30 (m, 2H, aliphatic chain). ^{13}C NMR (DMSO-d_6, 125 MHz) δ: 176.9, 171.8, 162.6, 161.4, 155.6, 145.0, 137.0, 128.2, 125.4, 124.7, 123.1, 122.7, 118.4, 115.0, 105.4, 67.1, 56.1, 48.9, 38.0, 34.9, 34.0, 28.3, 26.5, 25.5, 24.9. Anal. Calcd for $C_{30}H_{34}N_4O_4S_2$: C, 62.26; H, 5.92; N, 9.68. Found: C, 62.59; H, 5. 61; N, 9.53.

N-((1-(4-(4-(6-bromo-4-oxo-4H-chromen-2-yl)phenoxy)butyl)-1H-1,2,3-triazol-4-yl)methyl)-5-(1,2-dithiolan-3-yl)pentanamide (12) Off-white solid; mp 143–145 °C; IR (KBr, cm^{-1}) ν_{max}: 3303 (NH), 2929 (C-H), 1640 (C=O). ^1H NMR (DMSO-d_6, 500 MHz) δ: 8.27 (bt, 1H, NH), 8.09 (s, 1H, triazole) 8.05 (d, 2H, J = 8.5 Hz, phenoxy), 7.97 (d, 1H, J = 9.0 Hz, H_7), 7.91 (s, 1H, H_5), 7.78 (d, 1H, J = 9.0 Hz, H_8), 7.10 (d, 2H, J = 8.5 Hz, phenoxy), 7.00 (s, 1H, H_3), 4.43 (t, 2H, J = 6.5 Hz, CH$_2$-N), 4.28 (d, 2H, J = 5.5 Hz, CH$_2$-NH), 4.10 (t, 2H, J = 6.0 Hz, CH$_2$-O), 3.58–3.56 (m, 1H, CH-S), 3.19–3.08 (m, 2H, CH$_2$-S), 2.40–2.37 (m, 1H, S-CH$_2$-C$\underline{H}_2$), 2.09 (t, 2H, J = 7.0 Hz, CH$_2$-CO), 1.97 (t, 2H,

$J = 7.0$ Hz, C$\underline{H}_2$-CH$_2$-N), 1.85–1.82 (m, 1H, C$\underline{H}_2$-CH$_2$-S), 1.73–1.70 (m, 2H, O-CH$_2$-C$\underline{H}_2$), 1.65–1.62 (m, 1H, C$\underline{H}_2$-CH$_2$-CO), 1.51–1.50 (m, 3H, aliphatic chain), 1.33–1.30 (m, 2H, aliphatic chain). ^{13}C NMR (DMSO-d_6, 125 MHz) δ: 175.6, 171.9, 163.0, 161.6, 154.5, 145.0, 136.7, 128.4, 128.3, 126.9, 124.8, 122.8, 122.7, 121.1, 117.7, 115.0, 67.2, 56.1, 48.9, 38.0, 34.9, 34.0, 28.2, 26.5, 25.5, 24.9. Anal. Calcd for C$_{30}$H$_{33}$BrN$_4$O$_4$S$_2$: C, 54.79; H, 5.06; N, 8.52. Found: C, 55.09; H, 5.32; N, 8.43.

5-(1,2-Dithiolan-3-yl)-N-((1-(4-(4-(7-fluoro-4-oxo-4H-chromen-2-yl)phenoxy)butyl)-1H-1,2,3-triazol-4-yl)methyl)pentanamide (13) Off-white solid; mp 152–154 °C; IR (KBr, cm^{-1}) ν$_{max}$: 3309 (NH), 2928 (C-H), 1640 (C=O). ^{1}H NMR (DMSO-d_6, 500 MHz) δ: 8.27 (bs, 1H, NH), 8.10 (d, 1H, $J = 8.0$ Hz, H$_5$), 8.06 (d, 2H, $J = 8.0$ Hz, phenoxy), 7.92 (s, 1H, triazole), 7.73 (d, 1H, $J = 9.0$ Hz, H$_8$), 7.38 (t, 1H, $J = 8.0$ Hz, H$_6$), 7.10 (d, 2H, $J = 8.0$ Hz, phenoxy), 6.95 (s, 1H, H$_3$), 4.41 (t, 2H, $J = 6.5$ Hz, CH$_2$-N), 4.27 (d, 2H, $J = 5.5$ Hz, CH$_2$-NH), 4.10 (t, 2H, $J = 6.5$ Hz, CH$_2$-O), 3.60–3.55 (m, 1H, CH-S), 3.18–3.09 (m, 2H, CH$_2$-S), 2.41–2.36 (m, 1H, S-CH$_2$-C$\underline{H}_2$), 2.09 (t, 2H, $J = 7.0$ Hz, CH$_2$-CO), 1.99–1.96 (m, 2H, aliphatic chain), 1.85–1.81 (m, 1H, S-CH$_2$-C$\underline{H}_2$), 1.73–1.72 (m, 2H, aliphatic chain), 1.66–1.62 (m, 1H, C$\underline{H}_2$-CH$_2$-CO), 1.51–1.30 (m, 5H, aliphatic chain). ^{13}C NMR (DMSO-d_6, 125 MHz) δ: 176.1, 172.1, 163.3, 161.5, 154.2, 144.9, 128.2, 128.1, 122.8, 114.9, 107.5, 105.5, 67.2, 56.0, 48.8, 34.9, 34.0, 28.2, 26.5, 25.5, 24.9. Anal. Calcd for C$_{30}$H$_{33}$FN$_4$O$_4$S$_2$: C, 60.38; H, 5.57; N, 9.39. Found: C, 60.18; H, 5.31; N, 9.28.

N-((1-(4-(4-(6-chloro-4-oxo-4H-chromen-2-yl)phenoxy)butyl)-1H-1,2,3-triazol-4-yl)methyl)-5-(1,2-dithiolan-3-yl)pentanamide (14) Off-white solid; mp 142–144 °C; IR (KBr, cm^{-1}) ν$_{max}$: 3307 (NH), 2929 (C-H), 1630 (C=O). ^{1}H NMR (DMSO-d_6, 500 MHz) δ: 8.28 (t, 1H, $J = 5.5$ Hz, NH), 8.07 (d, 2H, $J = 8.5$ Hz, phenoxy), 7.96 (s, 1H, triazole), 7.92–7.86 (m, 3H, H$_5$, H$_7$ and H$_8$), 7.10 (d, 2H, $J = 8.5$ Hz, phenoxy), 7.00 (s, 1H, H$_3$), 4.41 (t, 2H, $J = 6.5$ Hz, CH$_2$-N), 4.28 (d, 2H, $J = 5.5$ Hz, CH$_2$-NH), 4.10 (t, 2H, $J = 6.5$ Hz, CH$_2$-O), 3.59–3.56 (m, 1H, CH-S), 3.19–3.07 (m, 2H, CH$_2$-S), 2.40–2.36 (m, 1H, S-CH$_2$-C$\underline{H}_2$), 2.09 (t, 2H, $J = 7.0$ Hz, CH$_2$-CO), 1.99–1.95 (m, 2H, C$\underline{H}_2$-CH$_2$-N), 1.85 (sextet, 1H, C$\underline{H}_2$-CH$_2$-S), 1.73–1.69 (m, 2H, C$\underline{H}_2$-CH$_2$-O), 1.65–1.62 (m, 1H, C$\underline{H}_2$-CH$_2$-CO), 1.53–1.50 (m, 3H, aliphatic chain), 1.35–1.30 (m, 2H, aliphatic chain). ^{13}C NMR (DMSO-d_6, 125 MHz) δ: 175.7, 171.8, 162.9, 161.6, 154.1, 150.4, 144.9, 133.9, 129.7, 128.4, 128.2, 124.4, 123.6, 122.8, 120.9, 115.0, 67.2, 56.1, 48.9, 38.0, 34.9, 34.0, 28.2, 26.5, 25.5, 24.9. Anal. Calcd for C$_{30}$H$_{33}$ClN$_4$O$_4$S$_2$: C, 58.76; H, 5.42; N, 9.14. Found: C, 58.61; H, 5.39; N, 9.36.

5-(1,2-Dithiolan-3-yl)-N-((1-(5-(4-(4-oxo-4H-chromen-2-yl)phenoxy)pentyl)-1H-1,2,3-triazol-4-yl)methyl)pentanamide (15) Off-white solid; mp 108–110 °C; IR (KBr, cm^{-1}) ν$_{max}$: 3301 (NH), 2928 (C-H), 1628 (C=O). ^{1}H NMR (DMSO-d_6, 500 MHz) δ: 8.24 (s, 1H, NH), 8.03 (m, 2H, phenoxy and H$_5$), 7.89 (s, 1H, triazole), 7.81 (t, 1H, $J = 8.0$ Hz, H$_7$), 7.76 (d, 1H, $J = 8.0$ Hz, H$_8$), 7.48 (t, 1H, $J = 8.0$ Hz, H$_6$), 7.08 (d, 2H, $J = 9.0$ Hz, phenoxy), 6.91(s, 1H, H$_3$), 4.36 (t, 2H, $J = 7.0$ Hz, CH$_2$-N), 4.28 (d, 2H, $J = 5.5$ Hz, CH$_2$-NH), 4.06 (t, 2H, $J = 6.5$ Hz, CH$_2$-O), 3.57 (quintet, $J = 6.0$ Hz, 1H, CH-S), 3.19–3.07 (m, 2H, S-CH$_2$), 2.39 (sextet, 1H, S-CH$_2$-C$\underline{H}_2$), 2.10 (t, 2H, $J = 7.5$ Hz, CH$_2$-CO), 1.88–1.76 (m, 5H, aliphatic chain), 1.65–1.60 (m, 1H, C$\underline{H}_2$-CH$_2$-CO), 1.54–1.50 (m, 3H, aliphatic chain), 1.42–1.31 (m, 4H, aliphatic chain). ^{13}C NMR (DMSO-d_6, 125 MHz) δ: 176.7, 171.7, 162.5, 161.4, 155.5, 144.8, 133.9, 128.0, 125.2, 424.6, 123.2, 123.0, 122.4, 118.2, 114.9, 105.3, 67.5, 56.0, 49.0, 39.7, 37.9, 34.9, 33.9, 29.3, 28.1, 27.7, 24.8. Anal. Calcd for C$_{31}$H$_{36}$N$_4$O$_4$S$_2$: C, 62.81; H, 6.12; N, 9.45. Found: C, 62.57; H, 5.86; N, 9.56.

N-((1-(5-(4-(6-bromo-4-oxo-4H-chromen-2-yl)phenoxy)pentyl)-1H-1,2,3-triazol-4-yl)methyl)-5-(1,2-dithiolan-3-yl)pentanamide (16) Off-white solid; mp 105–107 °C; IR (KBr, cm^{-1}) ν$_{max}$: 3310 (NH), 2927 (C-H), 1631 (C=O). ^{1}H NMR (DMSO-d_6, 500 MHz) δ: 8.26 (bs, 1H, NH), 8.09 (s, 1H, triazole), 8.05 (d, 2H, $J = 8.0$ Hz, phenoxy), 7.77 (d, 1H, $J = 9.0$ Hz, H$_7$), 7.88 (s, 1H, H$_5$), 7.77 (d, 1H, $J = 9.0$ Hz, H$_8$), 7.10 (d, 2H, $J = 8.0$ Hz, phenoxy), 6.99 (s, 1H, H$_3$), 4.35 (t, 2H, $J = 6.5$ Hz, CH$_2$-N), 4.28 (d, 2H, $J = 5.5$ Hz, CH$_2$-NH), 4.06 (t, 2H, $J = 6.5$ Hz, CH$_2$-O), 3.58–3.55 (m, 1H, CH-S), 3.19–3.09 (m, 2H, CH$_2$-S), 2.40–2.37 (m, 1H, S-CH$_2$-C$\underline{H}_2$), 2.08 (bs, 1H, CH$_2$-CO), 1.88–1.76 (m, 5H, aliphatic chain), 1.65–1.59 (m, 1H, C$\underline{H}_2$-CH$_2$-CO), 1.55–1.32 (m, 7H, aliphatic chain). ^{13}C NMR (DMSO-d_6, 125 MHz) δ: 175.6, 171.8, 162.9, 161.6, 156.2, 154.9, 144.9, 136.7, 130.4, 126.7, 128.3, 122.7, 121.1, 117.7, 114.9, 67.6, 56.1, 49.0, 34.9, 34.0, 29.4, 28.2, 27.8, 24.9, 22.0. Anal. Calcd for C$_{31}$H$_{36}$N$_4$O$_4$S$_2$: C, 55.43; H, 5.25; N, 8.34. Found: C, 55.23; H, 5.13; N, 8.04.

N-((1-(5-(4-(6-chloro-4-oxo-4H-chromen-2-yl)phenoxy)pentyl)-1H-1,2,3-triazol-4-yl)methyl)-5-(1,2-dithiolan-3-yl)pentanamide (17) Off-white solid; mp 140–142 °C; IR (KBr, cm^{-1}) ν$_{max}$: 3297 (NH), 2920 (C-H), 1630 (C=O). ^{1}H NMR (DMSO-d_6, 500 MHz) δ: 8.26 (bs, 1H, NH), 8.05 (d, 2H, $J = 8.0$ Hz, phenoxy), 7.96 (s, 1H, triazole), 7.89–7.85 (m, 3H, H$_5$, H$_7$ and H$_8$), 7.10 (d, 2H, $J = 8.0$ Hz, phenoxy), 6.99 (s, 1H, H$_3$), 4.35 (t, 2H, $J = 6.5$ Hz, CH$_2$-N), 4.28 (d, 2H, $J = 5.0$ Hz, CH$_2$-NH), 4.06 (t, 2H, $J = 6.0$ Hz, CH$_2$-O), 3.59–3.56 (m, 1H, CH-S), 3.18–3.08 (m, 2H, CH$_2$-S), 2.40–2.36 (m, 1H, S-CH$_2$-C$\underline{H}_2$), 2.09 (t, 2H, $J = 7.0$ Hz, CH$_2$-CO), 1.89–1.76 (m, 5H, aliphatic chain), 1.64–1.62 (m, 1H, C$\underline{H}_2$-CH$_2$-CO), 1.51–1.32 (m, 7H, aliphatic chain). ^{13}C NMR (DMSO-d_6, 125 MHz) δ: 175.7, 171.8, 161.6, 163.2, 157.2, 144.2, 129.7, 128.3, 128.2, 123.7, 122.7, 122.2, 114.9, 67.6, 56.3, 49.0, 38.1, 34.9, 34.0, 29.4, 28.2, 27.8, 24.9, 22.4. Anal. Calcd for C$_{31}$H$_{35}$ClN$_4$O$_4$S$_2$: C, 59.36; H, 5.62; N, 8.93. Found: C, 59.12; H, 5.29; N, 9.18.

5-(1,2-Dithiolan-3-yl)-N-((1-(3-((4-oxo-4H-chromen-7-yl)oxy)propyl)-1H-1,2,3-triazol-4-yl)methyl)pentanamide **(18)** Off-white solid; mp 89–91 °C; IR (KBr, cm^{-1}) ν_{max}: 3295 (NH), 2928 (C-H), 1640 (C=O). ^{1}H NMR (DMSO-d_6, 500 MHz) δ: 8.29 (t, 1H, $J = 5.5$ Hz, NH), 8.22 (d, 1H, $J = 6.0$ Hz, H$_5$), 7.94–7.92 (m, 2H, triazole and H$_2$), 7.11 (d, 1H, $J = 2.0$ Hz, H$_8$), 7.03 (dd, 1H, $J = 9.0$ Hz, $J = 2.5$ Hz, H$_6$), 6.26 (d, 1H, $J = 6.0$ Hz, H$_3$), 4.51 (t, 2H, $J = 7.0$ Hz, CH$_2$-N), 4.26 (d, 2H, $J = 5.5$ Hz, CH$_2$-NH), 4.11 (t, 2H, $J = 6.0$ Hz, CH$_2$-O), 3.60–3.54 (m, 1H, CH-S), 3.16–3.10 (m, 2H, CH$_2$-S), 2.41–2.36 (m, 1H, S-CH$_2$-C$\underline{H}_2$), 2.32–2.27 (m, 2H, aliphatic chain), 2.07 (t, 2H, $J = 7.5$ Hz, CH$_2$-CO), 1.85–1.82 (m, 1H, S-CH$_2$-C$\underline{H}_2$), 1.65–1.59 (m, 1H, C$\underline{H}_2$-CH$_2$-CO), 1.51–1.49 (m, 3H, aliphatic chain), 1.33–1.29 (m, 2H, aliphatic chain). ^{13}C NMR (DMSO-d_6, 125 MHz) δ: 175.6, 171.8, 162.7, 157.7, 145.1, 126.2, 118.1, 114.9, 114.8, 112.1, 101.3, 65.5, 56.1, 46.3, 38.1, 35.0, 34.1, 29.2, 28.3, 24.9. Anal. Calcd for C$_{23}$H$_{28}$N$_4$O$_4$S$_2$: C, 56.54; H, 5.78; N, 11.47. Found: C, 56.29; H, 6. 01; N, 11.55.

5-(1,2-Dithiolan-3-yl)-N-((1-(4-((4-oxo-4H-chromen-7-yl)oxy)butyl)-1H-1,2,3-triazol-4-yl)methyl)pentanamide **(19)** Off-white solid; mp 128–130 °C; IR (KBr, cm^{-1}) ν_{max}: 3296 (NH), 2927 (C-H), 1644 (C=O). ^{1}H NMR (DMSO-d_6, 500 MHz) δ: 8.30 (t, 1H, $J = 6.0$ Hz, NH), 8.10 (d, 1H, $J = 6.0$ Hz, H$_5$), 7.93–7.91 (m, 2H, triazole and H$_2$), 7.12 (d, 1H, $J = 2.5$ Hz, H$_8$), 7.04 (dd, 1H, $J = 8.5$ Hz, $J = 2.5$ Hz, H$_6$), 6.26 (d, 1H, $J = 6.0$ Hz, H$_3$), 4.40 (t, 2H, $J = 7.0$ Hz, CH$_2$-N), 4.26 (d, 2H, $J = 4.5$ Hz, CH$_2$-NH), 4.12 (t, 2H, $J = 6.5$ Hz, CH$_2$-O), 3.60–3.55 (m, 1H, CH-S), 3.18–3.08 (m, 2H, CH$_2$-S), 2.41–2.34 (m, 1H, S-CH$_2$-C$\underline{H}_2$), 2.08 (t, 2H, $J = 7.5$ Hz, CH$_2$-CO), 1.98–1.93 (m, 2H, aliphatic chain), 1.85–1.79 (m, 1H, S-CH$_2$-C$\underline{H}_2$), 1.74–1.68 (m, 2H, aliphatic chain), 1.66–1.60 (m, 1H, C$\underline{H}_2$-CH$_2$-CO), 1.55–1.47 (m, 3H, aliphatic chain), 1.34–1.29 (m, 2H, aliphatic chain). ^{13}C NMR (DMSO-d_6, 125 MHz) δ: 175.6, 171.9, 163.0, 156.5, 145.0, 122.1, 118.0, 114.9, 112.1, 101.4, 67.7, 56.1, 48.8, 38.1, 35.0, 34.1, 28.3, 26.5, 25.4, 24.9. Anal. Calcd for C$_{24}$H$_{30}$N$_4$O$_4$S$_2$: C, 57.35; H, 6.02; N, 11.15. Found: C, 57.28; H, 6. 33; N, 11.37.

5-(1,2-Dithiolan-3-yl)-N-((1-(5-((4-oxo-4H-chromen-7-yl)oxy)pentyl)-1H-1,2,3-triazol-4-yl)methyl)pentanamide **(20)** Off-white solid; mp 89–90 °C; IR (KBr, cm^{-1}) ν_{max}: 3296 (NH), 2929 (C-H), 1645 (C=O). ^{1}H NMR (DMSO-d_6, 500 MHz) δ: 8.29 (t, 1H, $J = 5.5$ Hz, NH), 8.21 (d, 1H, $J = 6.0$ Hz, H$_5$), 7.92–7.89 (m, 2H, triazole and H$_2$), 7.11 (d, 1H, $J = 2.0$ Hz, H$_8$), 7.02 (dd, 1H, $J = 8.8$ Hz, $J = 2.0$ Hz, H$_6$), 6.25 (d, 1H, $J = 6.0$ Hz, H$_3$), 4.34 (t, 2H, $J = 7.0$ Hz, CH$_2$-N), 4.26 (d, 2H, $J = 5.5$ Hz, CH$_2$-NH), 4.08 (t, 2H, $J = 6.2$ Hz, CH$_2$-O), 3.58–3.55 (m, 1H, CH-S), 3.18–3.08 (m, 2H, CH$_2$-S), 2.39–2.35 (m, 1H, S-CH$_2$-C$\underline{H}_2$), 2.08 (t, 2H, $J = 7.5$ Hz, CH$_2$-CO), 1.89–1.74 (m, 5H, aliphatic chain), 1.63–1.61 (m, 1H, C$\underline{H}_2$-CH$_2$-CO), 1.54–1.47 (m, 3H, aliphatic chain), 1.41–1.29 (m, 4H, aliphatic chain). ^{13}C NMR (DMSO-d_6, 125 MHz) δ: 175.6, 1718, 163.0, 147.7, 156.4, 144.9, 126.3, 122.3,

117.9, 114.9, 112.1, 101.2, 68.2, 56.1, 49.1, 38.0, 34.9, 34.0, 29.4, 28.3, 27.7, 24.9, 22.4. Anal. Calcd for C$_{25}$H$_{32}$N$_4$O$_4$S$_2$: C, 58.12; H, 6.24; N, 10.84. Found: C, 57.96; H, 6. 07; N, 10.53.

Biological assays

Neuroprotective activity of the compounds

The cell viability was evaluated with the colorimetric assay using 3-(4,5-dimethylthiazol-2-yl)-2,5-diphenyl tetrazolium bromide (MTT) [52]. PC12 cell line was obtained from the Iranian Biological Resource Center, IBRC. The seeded cells in 96-well plates (1×10^4 cells/well) were incubated for 24 h at 37 °C under a humidified air containing 5% CO$_2$. The cells were next treated with the tested compound (1–50 μM) and incubated for 3 h. Then, the cells were exposed with H$_2$O$_2$ (150 μM) and incubated for another 2 h. The medium was then replaced with 20 μL of MTT solution (5 mg/mL) and the cells were next incubated for another 4 h. The MTT solution was next removed and the crystals of formazan were solubilized using 100 μL of DMSO. A multi-mode plate reader (Biotek, Winooski, VT) was employed to record the appropriate absorbance at 570 nm. The results were reported as the percentage of untreated control cells and were the mean of three times determinations.

AChE/BuChE inhibition activity of the compounds

The Ellman method was used for ChE inhibition assay [53]. Donepezil was used as reference compound. The assay solution contained of phosphate buffer (0.1 M, pH 8.0), 5,5-dithiobis(2-nitrobenzoicacid) (0.01 M), *eel*AChE or *eq*BuChE (5 IU/mL, Sigma Chemical), various concentration of the tested compound solution and acetyl- or butyrylthiocholine iodide (0.05 M). The assay solutions in the presence or absence of the inhibitor were pre-incubated at 37 °C for 3 min after addition of the substrate. Each experiment was performed in triplicate, and log concentration versus inhibition curve was applied to achieve the IC$_{50}$ values graphically.

Determination of the inhibitory potency of the compound against Aβ$_{1-42}$ self-aggregation

Phosphate-buffered saline (PBS, pH 7.4, HyClone Thermo Scientific) having 1% ammonium hydroxide was utilized to solve Aβ$_{1-42}$ (50 μM, Sigma A9810). The solution was shaked for 72 h at 37 °C. Aliquot of Aβ$_{1-42}$ (10 μL) was incubated in PBS (0.05 M, pH 7.4) at 37 °C for 48 h with or without the tested inhibitor (100 μM). To investigate the Aβ$_{1-42}$ self-aggregation, the thioflavin T (ThT) fluorescence method was employed [54]. After incubation, the mixture was

treated with thioflavin T (50 μL, 200 μM, in 50 mM glycine-NaOH buffer, pH = 8.5). The amyloid fibril formation was screened by Microplate Reader (Spectra Max) at λ_{exc} = 448 nm and λ_{em} = 490 nm. Donepezil and rifampicin were applied as standard compounds. The inhibitory activity of the compound against Aβ-self-aggregation was calculated by the following equation: [(IFi/IFo) × 100] where IFi refers to the fluorescence intensity of Aβ$_{1-42}$ with inhibitor and IFo is related to the fluorescence intensity achieved for Aβ$_{1-42}$ in the absence of inhibitor.

Determination of intracellular ROS formation in PC12 cells induced by H$_2$O$_2$

The antioxidant potency of the selected compound was determined by measuring the amount of ROS evoked after PC12 cells exposure with H$_2$O$_2$. 2′,7′-dichloro-fluorescein diacetate (DCFH-DA) was employed as a ROS-sensitive dye to measure intracellular ROS formation [55]. PC12 cells seeded in 96-well plates were incubated at 37 °C in humidified CO$_2$ atmosphere (5%) for 24 h (1 × 10^4 cells/well in growth medium). The cells were then exposed with the tested compound (1–50 μM) for 6 h. After cell washing with PBS, the cells were incubated with 150 μM of H$_2$O$_2$ for 18 h. After washing the cells with PBS, they were incubated with 10 μM of DCFH-DA for 30 min at 37 °C under dark. The fluorescence of the DCF in the cells was calculated using ELISA spectrofluorometer (BioTek, excitation/emission at 485 nm/528 nm) after removal of DCFH-DA and washing the cells with PBS. The results are the percentage of increase in intracellular ROS compared to the control (untreated cells) and calculated by the formula [(F$_t$ − F$_{nt}$)/F$_{nt}$ × 100], where F$_t$ = fluorescence of the treated cells and F$_{nt}$ = fluorescence of untreated cells.

FRAP assay

Previously reported method with slight modifications was used to determine the total antioxidant power of the compound [56]. A 240 μL of FRAP reagent (a mixture of three solutions containing 20 mM FeCl$_3$, 10 mM TPTZ (2,4,6-tripyridyl-s-triazine), and 0.3 M acetate buffer having pH of 3.6) was added to the selected compound (10 μL, 10 μM) and the obtained solution was incubated for 15 min. The changes in the absorbance was studied by a microplate reader (BioTek Synergy HT) at 593 nm and the proportion of Fe^{3+} reduced to Fe^{2+} concentration was then calculated according to the plotted standard curve of Fe^{2+}.

Metal chelating ability

The metal chelation activity of the selected compound was studied in the presence and absence of bio-metal ions (FeSO$_4$, CuCl$_2$, MgCl$_2$, ZnCl$_2$, CaCl$_2$, and AlCl$_3$). The tested compound was incubated with various concentrations metal ions for 0.5 h at ambient temperature and the appropriate spectrum was taken by a dual-beam (GBC Cintra 101) spectrophotometer in the range of wavelength from 200 to 500 nm. The stoichiometry of the complex was determined using the molar ratio method. UV-vis spectra of metal solution (2.5 mL, 80 μM) at increasing ligand concentrations were recorded [57].

Docking simulation

The Autodock vina software 1-1-2 and the AChE and BuChE crystal structure (PDB cod: 1EVE and 4BDS, respectively) was used for docking study. The conversion of the ligand to pdbqt format was conducted by Open babel (2.3.1) [58]. The active site dimensions were set as box size: 20 × 20 × 20 Å. Molecular visualization was carried out by DS visualizer molecular graphics system [59].

Statistical analysis

Data were expressed as mean ± standard error of the mean (SEM) of the experiments (at least three independent measurements). One-way ANOVA with Dunnett post hoc test was used for statistical analysis and a p value less than 0.05 was considered statistically significant.

Results and discussion

Chemistry

As illustrated in Scheme 1, compound 3 was initially synthesized via reaction of substituted 2′-hydroxyacetophenone with 4-methoxy benzaldehyde through a domino aldol-Michael-oxidation reaction catalyzed by pyrrolidine and iodine in dimethyl sulfoxide (DMSO). Compound 3 was converted to the corresponding 2-(4-hydroxyphenyl)-4H-chromen-4-one derivatives (4a-d) by BBr$_3$ in dichloromethane. Compound 5 was also prepared in one step from the reaction of 2,4-dihydroxyacetophenone and triethyl orthoformate in the present of 70% perchloric acid leading to the formation of perchlorate salt which was then hydrolyzed to reach target compound (5). The bromoalkoxy intermediates 6a-i, and 8a-c were then prepared via the reaction of 4a-d or 5 with appropriate amount of dibromoalkanes in acetone solution of anhydrous K$_2$CO$_3$ under refluxing condition for 4 h. Compound 7 was separately synthesized through the amidation reaction between LA and propargylamine in the presence of 4-dimethylaminopyridine (DMAP) and N,N'-dicyclohexylcarbodiimide (EDCI). Target compounds 9–20 were finally prepared through a one-pot three-component
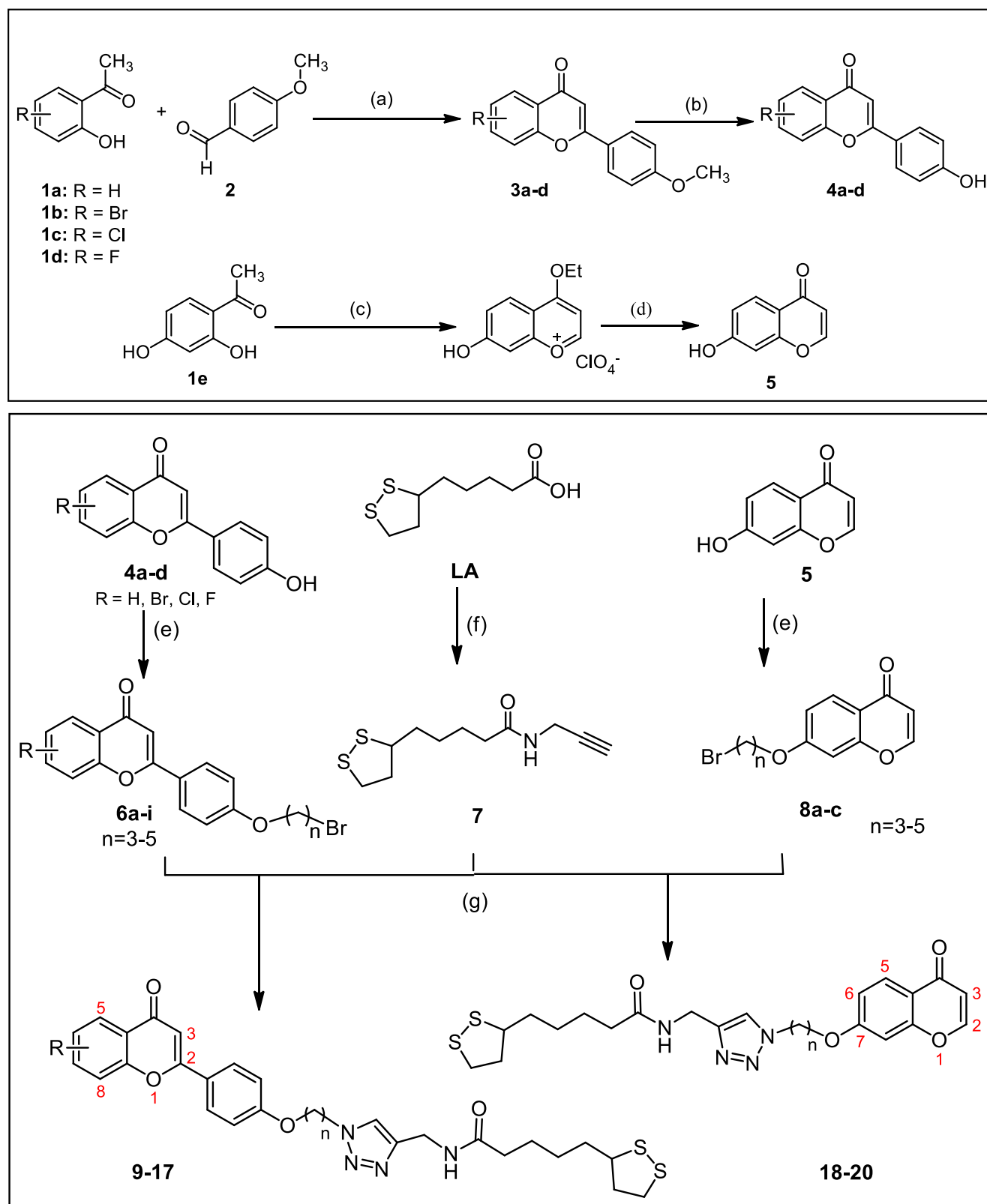
Scheme 1 Synthetic routes to compounds 9–20. Reagents and conditions: (**a**) pyrrolidine, DMSO, I$_2$; (**b**) BBr$_3$, DCM; (**c**) HC(OEt)$_3$, 70% HClO$_4$; (**d**) H$_2$O, 100 °C; (**e**) Br(CH)$_n$Br (*n* = 3–5), anhydrous K$_2$CO$_3$, acetone, reflux, 4 h; (**f**) propargylamine, EDCI, DMAP, CH$_2$Cl$_2$, rt., 12 h; (**g**) NaN$_3$, CuSO$_4$, sodium ascorbate, t-Butanol/H$_2$O, 70 °C, 12 h

reaction between compounds **6a-i** or **8a-c**, sodium azide and compound **7** catalyzed by copper (II).

Biological assay

Primarily, neuroprotection and cholinesterase inhibitory activities of all target compounds **9–20** were evaluated to find the best potent compound for further studies.

Neuroprotection potency against PC12 cell damaged induced by H_2O_2

Oxidative damage and neurotoxicity created by H_2O_2 are considered as most important factor controlling the progress of neurodegenerative disorder [60]. Therefore, neuroprotection activity of the prepared chromone–LA conjugates **9–20** were screened at different concentrations of 1, 5, 10, 20 and 50 μM

using MTT assay. All compounds, in all concentrations, could significantly increase the cell viability of PC12 cells dose dependently, even at low concentration of 1 μM (Table 1, $p < 0.001$). Interestingly, compounds **15**, **16**, and **17** having five carbon chain length ($n = 5$) exhibited higher neuroprotective activity than that of quercetin as reference drug in all concentrations. By comparison between compounds **9**, **11**, and **15** bearing simple 2-phenyl-4H-chromen-4-one moiety and different carbon chain length ($n = 3$, 4 and 5 for compounds **9**, **11**, and **15**, respectively), it could be implied that increasing the size of cross-linker could increase the neuroprotection activity of the target compounds (Table 1). The same behaviour was also seen for compounds **18–20** as 4H-chromen-4-one derivatives substituted at 7 position. Notably, the unsubstituted chromen derivatives had less neuroprotective activity on the H_2O_2-induced cell death than halo-substituted analogues (compare compound **9** with compound
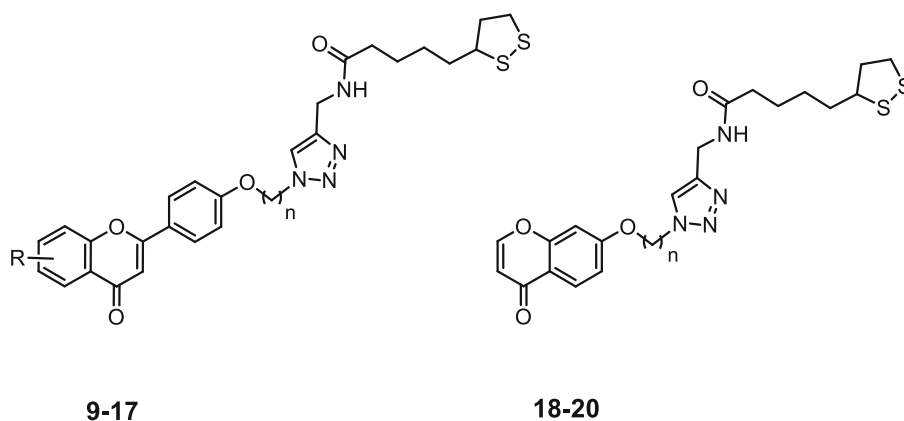

9-17   **18-20**

Table 1 The protective effect of compounds 9–20 against H_2O_2-induced injury in PC12 cell line at different concentrations

Compound	n	R	PC12 cells viability (% of control)[a]					
			H_2O_2	1 μM	5 μM	10 μM	20 μM	50 μM
9	3	H	22.2 ± 2.1	28.1 ± 1.6[***]	32.4 ± 2.6[***]	36.0 ± 1.8[***]	37.2 ± 1.5[***]	38.5 ± 1.7[***]
10	3	6-Br	20.1 ± 1.2	31.3 ± 1.0[***]	33.5 ± 0.9[***]	40.5 ± 0.9[***]	43.8 ± 1.0[***]	48.1 ± 1.1[***]
11	4	H	25.0 ± 1.4	33.0 ± 1.2[***]	39.3 ± 0.8[***]	41.3 ± 1.2[***]	44.2 ± 0.8[***]	46..5 ± 1.2[***]
12	4	6-Br	26.6 ± 0.5	38.3 ± 1.0[***]	48.9 ± 1.2[***]	52.8 ± 0.5[***]	59.3 ± 0.6[***]	64.3 ± 1.4[***]
13	4	7-F	24.7 ± 1.4	37.2 ± 0.6[***]	41.0 ± 1.0[***]	48.3 ± 2.0[***]	53.0 ± 2.6[***]	59.7 ± 2.2[***]
14	4	6-Cl	24.6 ± 0.2	38.8 ± 0.8[***]	44.7 ± 0.5[***]	50.5 ± 0.6[***]	60.9 ± 0.6[***]	66.4 ± 1.0[***]
15	5	H	25.8 ± 1.1	44.9 ± 1.2[***]	52.0 ± 1.1[***]	57.2 ± 0.7[***]	61.6 ± 1.1[***]	65.2 ± 0.2[***]
16	5	6-Br	25.9 ± 1.3	47.7 ± 1.0[***]	59.0 ± 0.8[***]	67.8 ± 0.6[***]	71.6 ± 1.6[***]	81.8 ± 1.2[***]
17	5	6-Cl	25.9 ± 0.9	44.9 ± 0.6[***]	52.8 ± 0.7[***]	60.8 ± 1.1[***]	69.3 ± 0.7[***]	75.3 ± 1.4[***]
18	3	–	22.8 ± 1.2	28.3 ± 0.9[***]	31.0 ± 2.1[***]	36.7 ± 1.1[***]	40.1 ± 0.9[***]	43.4 ± 0.5[***]
19	4	–	27.5 ± 1.0	35.6 ± 0.3[***]	42.8 ± 0.7[***]	45.4 ± 1.2[***]	50.2 ± 0.6[***]	53.9 ± 0.1[***]
20	5	–	28.0 ± 0.4	41.0 ± 0.3[***]	47.2 ± 0.5[***]	52.3 ± 0.5[***]	57.4 ± 0.5[***]	62.5 ± 0.8[***]
Quercetin	–	–	28.6 ± 0.8	40.7 ± 0.4[***]	47.3 ± 0.9[***]	53.7 ± 1.2[***]	56.9 ± 0.5[***]	58.8 ± 0.1[***]

[a)][***] Cell viability was determined using MTT assay protocol. Data are expressed as the mean ± SEM of three independent replicates. The significant ($p < 0.001$) values with respect to the H_2O_2 group

10, compound **11** with compounds **12**–**14** and compound **15** with compounds **16** and even **17** at especially high concentrations).

Cholinesterase inhibitory activity

AChE and BuChE inhibitory activity of all chromone–LA conjugates **9**–**20** were investigated. Table 2 shows the IC_{50} values of the compounds compared with standard drug donepezil. No significant effect was observed against AChE at 100 μM for most of the compounds, except 7-fluoro derivative (**13**) with moderate activity against AChE (IC_{50} = 56.50 μM). The results revealed that the activity of the 7-position substituted derivatives (**18**–**20**) against BuChE was better than the 2-position modified derivatives (**9**–**17**). Among the 7-substituted derivatives, only compound **18** and **19** with 3 or 4 atom chain lengths showed appropriate anti-BuChE activity (IC_{50} = 15.32 and 7.55 μM, respectively). Compound **20** with 5 carbone spacer (n = 5) revealed no activity against

BuChE confirming the great effect of the cross-linker and size of the molecule to occupy the enzyme active site. Therefore, the extension of the linker has no positive effect on the BuChE inhibitory potency.

When tacrin bearing halogen substituent was conjugated to LA by 3 carbone spacer, the AChE and BuChE inhibition activities, especially AChEI activity, were improved in comparison with tacrin [35]. The study confirmed the important role of the length of the cross-linker on ChEs inhibition activity of the target compounds. Previous study also revealed that hybridization of tacrin with chromone scaffold improves BuChE inhibition activity more than that of AChEI which is in good agreement with the achievement of our results [30]. The same result was also observed when other well-known pharmacophores combine with each other. Attachment of LA and/or chromone to rivastigmine resulted in a higher BuChE inhibition activity than AChE inhibition [28]. It seems that LA can improve the
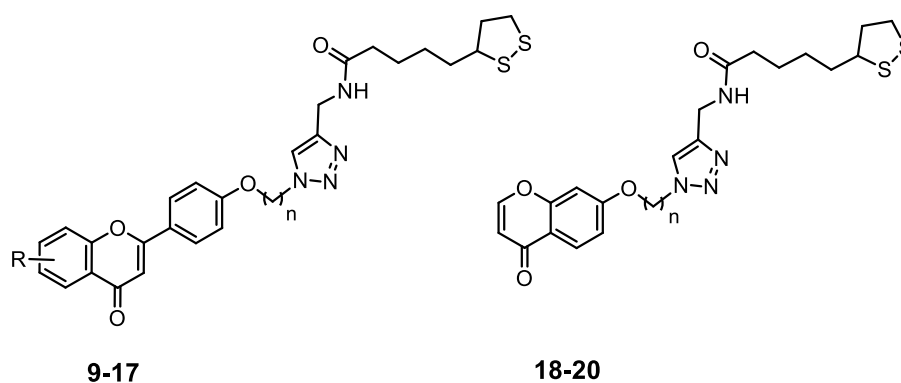

9-17   **18-20**

Table 2 Inhibitory activity of the synthesized compounds 9–20 against AChE and BuChE

Compound	n	R	AChE[a] IC_{50} (μM)	BuChE[a] IC_{50} (μM)
9	3	H	>100	>100
10	3	6-Br	>100	>100
11	4	H	>100	>100
12	4	6-Br	>100	>100
13	4	7-F	56.50 ± 3.91	>100
14	4	6-Cl	>100	>100
15	5	H	>100	>100
16	5	6-Br	>100	>100
17	5	6-Cl	>100	>100
18	3	–	>100	15.32 ± 1.21
19	4	–	>100	7.55 ± 0.78
20	5	–	>100	>100
Donepezil	–	–	0.027 ± 0.004	4.01 ± 0.56

[a] Inhibitor concentration (mean ± SEM of three experiments) required for 50% inactivation of ChE

BuChE inhibition activity of the mother scaffold more than AChE inhibition activity. Based on the results, it seems that electron donating groups on chromone scaffold and also using appropriate spacer to prevent molecular folding may facilitate proper interactions with the enzyme transforming target compounds into more potent inhibitors.

Other biological evaluation for the selected compound (19)

The neuroprotection assay revealed that all compounds could significantly protect PC12 cells against oxidative damage. However, among all chromone–LA conjugates, only compounds **13**, **18** and **19** showed moderate anti-ChE activity. Also, compound **19** exhibited more potent neuroprotective activity (comparable with quercetin as reference drug) and the highest anti-BuChE activity. Therefore, all other studies were performed for compound **19**.

Kinetic analysis of BuChE inhibition

The kinetic study of the most active anti-BuChE compound **19** was evaluated at different concentrations of the substrate. Lineweaver-Burk plots confirmed mixed-type of inhibition against BuChE (Fig. 2a) suggesting the ability of compound **19** to interact with both catalytic active site (CAS) and peripheral anionic site (PAS) of the enzyme. The inhibition constant Ki was calculated (Ki = 7.97 μM) and a non-competitive inhibition was obtained from secondary plots of the slope versus concentration of compound **19** (Fig. 2b).

Docking studies

The binding modes of the most active compounds against AChE (**13**) and BuChE (**19**) in the active site of the enzymes were defined by docking study. According to the docking scores, the binding energies of −10.60 Kcal/mol and −9.32 Kcal/mol were calculated for **13** and **19** in the active site of AChE, respectively. The lower affinity of compound **19** in the AChE active site could be attributed to the lack of suitable interaction with PAS of the enzyme. In contrast, two stabilizing π-π stacking with Trp 279 could be occurred for compound **13**. As depicted in Fig. 3, both molecules have folded to accommodate in the enzymes active site. The π-sulfur interaction between 1,2-dithiolane and central triazole ring stabilized the conformation. Moreover, an extra π-sulfur interaction between 1,2-dithiolane and Trp 84 and Phe 330 were observed. In this orientation, the more lipophilic part of the molecule tends to bind with PAS. The folding of the molecule has closed up the benzopyranone ring to the PAS. In such conformation, π-π stacking could be formed with Trp 279. This π-π stacking is crucial to discriminate between **13** and **19** to bind more tightly to the active site.

In the case of BuChE, compounds **13** and **19** expressed different modes of binding in such a way that the folding of the molecules was quite different. In both molecules the triazole ring served as hinge to help molecule forming U-shape. As can be seen in Fig. 4, compound **19** folded outside the gorge; while, compound **13** folded inside. The binding energies were −8.89 and −8.43 for compounds **19** and **13**, respectively. The less binding energy of compound **13** could be explained by more conformational energy and steric hindrance with the receptor.
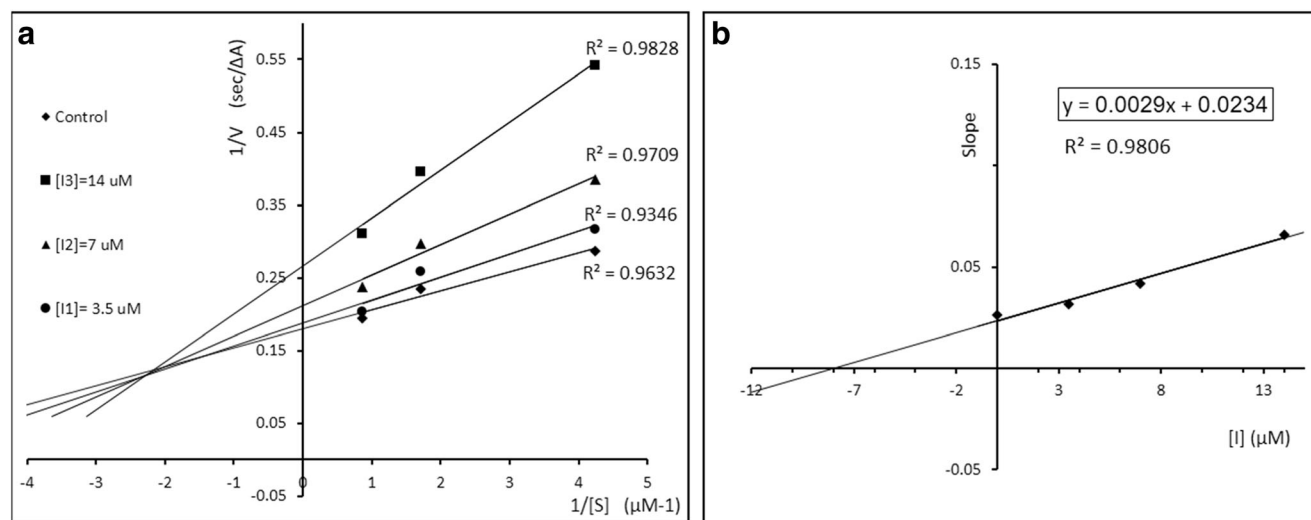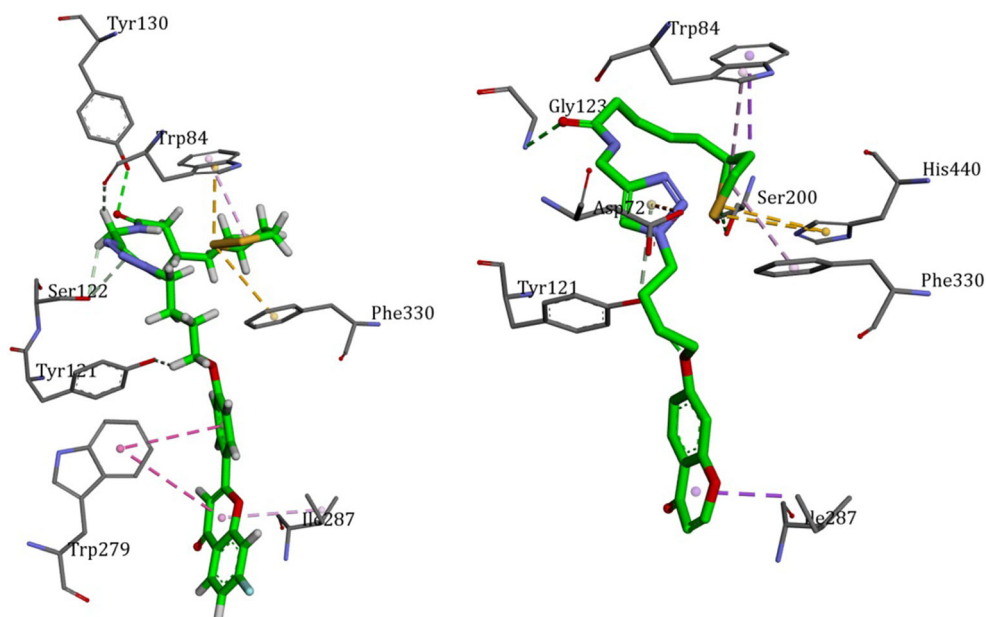

Fig. 2 **a** Lineweaver-Burk plot for the inhibition of BuChE by compound 19 at different concentrations of BuTCh, (**b**) Secondary plot for calculation of steady-state inhibition constant of compound 19, $K_i = 7.97$ μM

Anti-amyloid aggregation activity

According to the role of BuChE in Aβ formation [5], the ability of compound **19**, as most active BuChEI, against amyloid-beta aggregation was determined using the thioflavin T (ThT) analysis and compared with standard drugs (donepezil and rifampicin). The results in Table 3 show that compound **19** display moderate potency (13% inhibition, at 100 μM concentration), in comparison to donepezil (22% at 100 μM concentration) to inhibit Aβ aggregation. This reduced inhibitory ability compared to our previous coumarin-LA adducts with 62.4% and 51.2% inhibition activity [14], could be probably due to the absence of electron-donating

functional groups (specially methoxy group) on compound **19** and also lack of appropriate hydrophobic and aromatic interactions between Aβ probes and inhibitor [61].

Intracellular ROS inhibition activity of the selected compound

DCFH-DA (Dichloro-dihydro-fluorescein diacetate) assay was applied to investigate the antioxidant activity of compound **19** against intracellular ROS formation in PC12 cells at concentrations having no effect on the cell viability (1, 5, 10 and 50 μM). The results revealed that ROS production significantly decreased in a
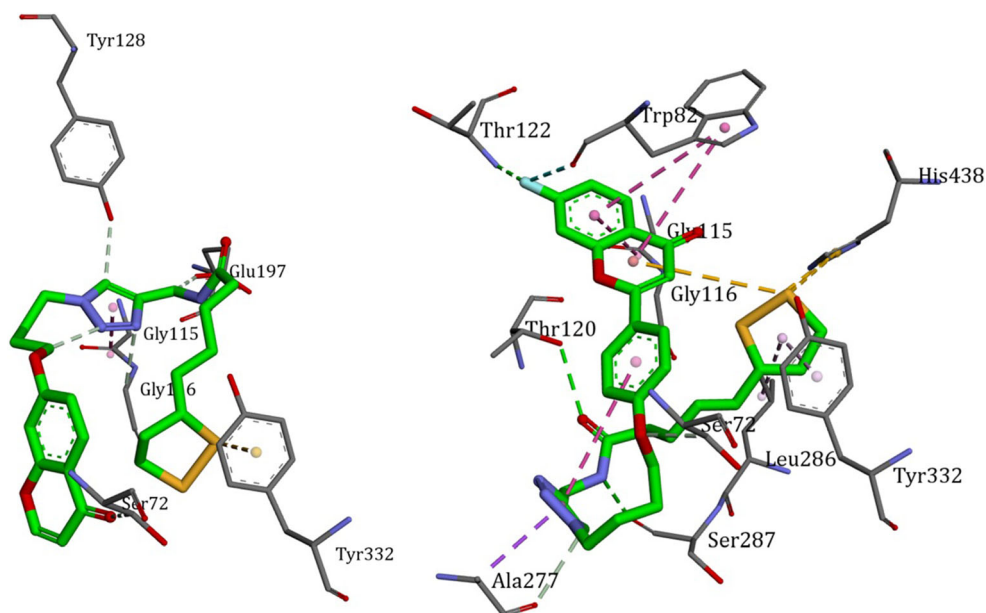
Table 3 Inhibition of Aβ self-aggregation by the compound **19**

Compound	Inhibition of Aβ Self-aggregation[a] (%)
19	13.1 ± 3.2
Rifampicin	27.5 ± 4.3
Donepezil	22 ± 5.4

[a] $A\beta_{1-42}$ (10 μM) aggregation in presence of the tested compound (100 μM)

concentration-independent manner (Fig. 5, Table S1). In concentration of 10 μM, ROS formation was significantly lower than the H_2O_2 group, while LA showed similar inhibition activity at the higher concentration (50 μM). Moreover, the endogenous ROS significantly decreased in the treated cells with compound **19** compared with untreated control cells. Beside antioxidant effects of LA part, the presence of an α,β-unsaturated carbonyl group in chromone scaffold could have a complementary effect on the antioxidant activity. Based on previous reports, it seems that the presence of electron donating groups like hydroxyl and methoxy group can improve the antioxidant activity of the target compounds [36].

Total antioxidant assay

The FRAP (ferric reducing antioxidant power) of the compound **19** was compared with LA, quercetin, and ascorbic acid. The results indicated that compound **19** have excellent reducing power (Fe^{+2}, 85.57 mM), comparable with quercetin and LA (Table 4) and could be considered as strong antioxidant.

Metal-chelating property

The chelating ability of compound **19** towards biologically relevant metal ions (Cu^{+2}, Fe^{+2}, Ca^{+2}, Mg^{+2}, Zn^{+2}, and Al^{+3}) was investigated by UV-vis spectrometry (Fig. 6a). In the absence of metal ions, the spectrum of compound **19** showed the maximum absorption at 303, and 297 nm. The curve intensity increased when $CuCl_2$ was added suggesting the formation of 19-Cu^{2+} complex. However, no significant change was observed in the UV spectrum after adding $FeSO_4$, $CaCl_2$, $MgCl_2$, $ZnCl_2$ or $AlCl_3$. The ability of compound **19** to chelate Cu^{2+} as bio-metal was studied by using mole ratio method. In this method, the total molar concentration of the tested ligand was continuously varied, while the molar concentration of Cu(II) was kept constant. As indicated in Fig. 6b, the addition of compound **19** to Cu^{+2} leads to an increase in the maximum absorbance
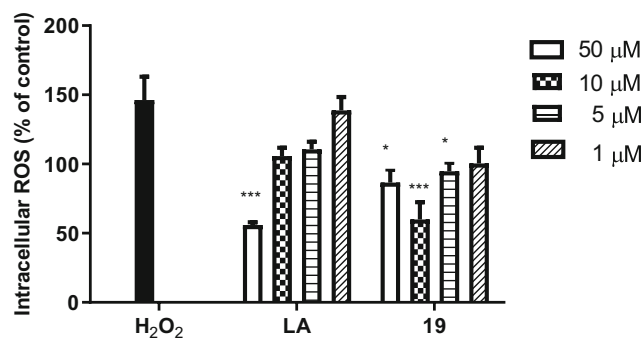

Fig. 5 The effect of compound **19** and LA on intracellular ROS formation in neuronal PC12 cells. Values are the mean $\pm$ SEM of three independent experiments ($^*P < 0.05$, $^{***}P < 0.001$) vs. H_2O_2 group (See supporting information for details, Table S1)

which was then plateaued at a mole ratio of 2, indicating a 2:1 stoichiometry for complex of **19**-copper ions. The presence of several chelating sites including amid and disulfide bonds on the target compounds is one of the reasons why compound **19** turn into great antioxidant.

Conclusion

In summary, a new series of chromone-LA hybrids were introduced as multifunctional agents against AD. All target compounds were potent as neuroprotective agents against H_2O_2-induced cell death. Especially, compounds **15**, **16**, and **17** were more active than quercetin (reference drug) in all range of concentrations. The anti-ChE assay showed that only 7-fluoro-flavone derivative **13** has moderate activity against AChE. In the case of BuChE inhibition, 7-position substituted derivatives showed more inhibitory activity than 2-position modified compounds. Among the 7-position substituted congeners, only compounds **18** and **19** showed proper BuChE inhibitory activity ($IC_{50} = 15.32$ and 7.55 μM, respectively). It could be eventually concluded that the chromone-LA hybrids showed significant neuroprotective activity in all concentrations, especially in halo- or methoxy-substituted derivatives. In the case of anti-

Table 4 Antioxidant activity of compound 19 determined by FRAP assay

Compound	FRAP (mM)[a]
19	85.57 ± 0.61
Lipoic acid	84.23 ± 0.79
Ascorbic acid	81.16 ± 0.50
Quercetin	84.77 ± 1.18

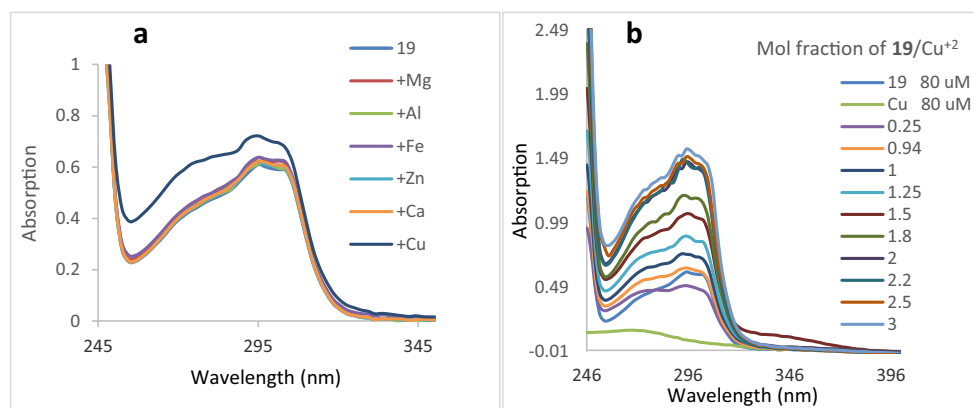[a] The data are expressed as Mean $\pm$ SEM of three experiments

Fig. 6 a The UV spectra of compound 19 (final concentration, 80 μM in methanol) alone or in the presence of MgCl$_2$, AlCl$_3$, FeSO$_4$, ZnCl$_2$, CaCl$_2$, and CuCl$_2$ (final concentration, 80 μM in methanol). **b** Determination of the stoichiometry of Cu^{+2}-19 complex using molar ratio method through titrating the methanol solution of CuCl$_2$ (80 μM) with ascending amounts of compound 19 (1000 μM in methanol, titration step 0.01 mL)

ChE activity, most of the compounds were weak inhibitors of AChE and BChE, suggesting that further studies are needed on the chromone substitution and the length of the cross-linker. It seems that changing the substituents on the chromone scaffold may improve the BuChE inhibition activity of the target compound through well matching with the active site of the enzymes. However, the main aim of this work was to make a balanced in multi-target profile of the target compound rather than finding high potent ChE inhibitor. In modern medicinal chemistry, "one-molecule, one-target" paradigm has been replaced with MTDL approach leading to simplify the drug discovery process and generation of novel and efficient multi-target small molecules against AD. Some studies suggested that MTDLs with the mild activity against one or several targets may result in better in vivo outcomes compared to the one-target compounds having high affinity. Since week connections mostly control cellular networks, low-affinity MTDLs may be enough to create the significant results.

The novel chromone-LA hybrid (compound **19**) introduced in this work, could be considered as potent neuroprotective agent having selective copper chelation ability with good BuChE inhibition activity and moderate anti-amyloid aggregation potency. More study on the effect of the substituent on chromone scaffold and the type and length of the cross-linker would be the future objective of the work.

Author's contributions Leili Jalili-Baleh synthesized and characterized the compounds and participated in the writing of the manuscript. Hamid Nadri evaluated ChEs inhibition activity of the compounds, docking and kinetic studies. Hamid Forootanfar evaluated neuroprotective activity of the compounds. Tuba Tüylü Küçükkılınç and Beyza Ayazgök participated in intracellular ROS inhibition activity of the compound. Mahban Rahimifard and Maryam Baeeri performed FRAP assay. Mohammad Sharifzadeh, Mohammad Abdollahi and Alireza Foroumadi contributed to the characterization of the compounds, data analysis and revision of the manuscript. Mehdi Khoobi conceived the main idea of the study, organized the work and contributed to the overall analysis of the results. All the authors reviewed and approved the manuscript.

Compliance with ethical standards

Conflict of interest   The authors have declared no conflict of interest.

References

1. Querfurth HW, Laferla FM. Alzheimer's disease. N Engl J Med. 2010;362:329–44.

2. Kumar A, Ekavali AS. A review on Alzheimer's disease pathophysiology and its management: an update. Pharmacol Rep. 2015;67:195–203.

3. Cheignon C, Tomas M, Bonnefont-Rousselot D, Faller P, Hureau C, Collin F. Oxidative stress and the amyloid beta peptide in Alzheimer's disease. Redox Biol. 2018;14:450–64.

4. Zhang FQ, Jiang JL, Zhang JT, Niu H, Fu XQ, Zeng LL. Current status and future prospects of stem cell therapy in Alzheimer's disease. Neural Regen Res. 2020;15:242–50.

5. Nilsson P, Iwata N, Muramatsu S, Tjernberg LO, Winblad B, Saido TC. Gene therapy in Alzheimer's disease-potential for disease modification. J Cell Mol Med. 2010;14:741–57.

6. Mushtaq G, Greig NH, Khan JA, Kamal MA. Status of acetylcholinesterase and butyrylcholinesterase in Alzheimer's disease and type 2 diabetes mellitus. CNS Neurol Disord Drug Targets. 2014;13:1432–9.

7. Darvesh S, Cash MK, Reid GA, Martin E, Mitnitski A, Geula C. Butyrylcholinesterase is associated with β-amyloid plaques in the transgenic APPSWE/PSEN1dE9 mouse model of Alzheimer disease. J Neuropathol Exp Neurol. 2012;71:2–14.

8. Podoly E, Hanin G, Soreq H. Alanine-to-threonine substitutions and amyloid diseases: butyrylcholinesterase as a case study. Chem Biol Interact. 2010;187:64–71.

9. Liu Z, Zhang A, Sun H, Han Y, Kong L, Wang X. Two decades of new drug discovery and development for Alzheimer's disease. RSC Adv. 2017;7:6046–58.

10. Cavalli A, Bolognesi ML, Minarini A, Rosini M, Tumiatti V, Recanatini M, Melchiorre C. Multi-target-directed ligands to combat neurodegenerative diseases. J Med Chem. 2008;51:347–72.

11. Jesus Oset-Gasque M, Marco-Contelles J. Alzheimer's disease, the "One-Molecule, One-Target" paradigm, and the multitarget directed ligand approach. ACS Chem Neurosci. 2018;9:401–3.

12. Wenzel TJ, Klegeris A. Novel multi-target directed ligand-based strategies for reducing neuroinflammation in Alzheimer's disease. Life Sci. 2018;15:314–22.

13. Blaikie L, Kay G, Thoo Lin PK. Current and emerging therapeutic targets of alzheimer's disease for the design of multi-target directed ligands. Med Chem Commun. 2019;10:2052–72.

14. Ibrahim MM, Gabr MT. Multitarget therapeutic strategies for Alzheimer's disease. Neural Regen Res. 2019;14(3):437–40.

15. Jalili-Baleh L, Nadri H, Forootanfar H, Samzadeh-Kermani A, Tüylü Küçükkılınç T, Ayazgok B, Rahimifard M, Baeeri M, Doostmohammadi M, Firoozpour L, et al. Novel 3-phenylcoumarin–lipoic acid conjugates as multi-functional agents for potential treatment of Alzheimer's disease. Bioorg Chem. 2018a;79:223–34.

16. Jalili-Baleh L, Forootanfar H, Tüylü Küçükkılınç T, Nadri H, Abdolahi Z, Ameri A, Jafari M, Ayazgok B, Baeeri M, Rahimifard M, SNA B, et al. Design, synthesis and evaluation of novel multi-target-directed ligands for treatment of Alzheimer's disease based on coumarin and lipoic acid scaffolds. Eur J Med Chem. 2018b;152:600–14.

17. de Freitas SM, Dias KST, Gontijo VS, Ortiz CJC, Viegas C Jr. Multi-target directed drugs as a modern approach for drug design towards Alzheimer's disease: an update. Curr Med Chem. 2018;25:3491–525.

18. Keri RS, Quintanova C, Chaves S, Silva DF, Cardoso SM, Santos MA. New tacrine hybrids with natural-based cysteine derivatives as multi targeted drugs for potential treatment of Alzheimer's disease. Chem Boil Drug Des. 2016a;87:101–11.

19. Choudhary S, Kumar Singh P, Verma H, Singh H, Silakari O. Success stories of natural product-based hybrid molecules for multifactorial diseases. Eur J Med Chem. 2018b;151:62–97.

20. Reis J, Gaspar A, Milhazes N, Borges F. Chromone as a privileged scaffold in drug discovery: recent advances. J Med Chem. 2017;60(19):7941–57.

21. Pachón-Angona I, Refouvelet B, Andrýs R, Martin H, Luzet V, Iriepa I, Moraleda I, Diez-Iriepa D, Oset-Gasque MJ, Marco-Contelles J, Musilek K, Ismaili L. Donepezil+chromone+melatonin hybrids as promising agents for Alzheimer's disease therapy. J Enzy Inhib Med Chem. 2019;34(1):479–89.

22. Kumar S, Mishra A, Pandey AK. Antioxidant mediated protective effect of Parthenium hysterophorus against oxidative damage using in vitro models. BMC Compl Altern Med. 2013;13:120.

23. Kumar S, Pandey AK. Phenolic content, reducing power and membrane protective activities of Solanum xanthocarpum root extracts. Int J Plant Res. 2013;26:301–7.

24. Leopoldini M, Russo N, Chiodo S, Toscano M. Iron chelation by the powerful antioxidant flavonoid quercetin. J Agricul Food Chem. 2006;54:6343–51.

25. Reis J, Cagide F, Valencia ME, Teixeira J, Bagetta D, Pérez C, Uriarte E, Oliveira PJ, Ortuso F, Alcaro S, Rodríguez-Franco MI, Borges F. Multi-target-directed ligands for Alzheimer's disease: discovery of chromone-based monoamine oxidase/cholinesterase inhibitors. Eur J Med Chem. 2018;158:781–800.

26. Cruz I, Puthongking P, Cravo S, et al. Xanthone and flavone derivatives as dual agents with acetylcholinesterase inhibition and antioxidant activity as potential anti-alzheimer agents. J Chem. 2017;2017:e8587260.

27. Vauzour D, Vafeiadou K, Rodriguez-Mateos A, Rendeiro C, Spencer JPE. The neuroprotective potential of flavonoids: a multiplicity of effects. Gene Nutr. 2008;3:115–26.

28. Nabavi SF, Braidy N, Habtemariam S, Orhan IE, Daglia M, Manayi A, Gortzi O, Nabavi SM. Neuroprotective effects of chrysin: from chemistry to medicine. Neurochem Int. 2015;90:224–31.

29. Gautam R, Jachak SM, Kumar V, Mohan CG. Synthesis, biological evaluation and molecular docking studies of stellatin derivatives a cyclooxygenase (COX-1, COX-2) inhibitors and anti-inflammatory agents. Bioorg Med Chem Lett. 2011;21:1612–6.

30. Nesi G, Chen Q, Sestito S, Digiacomo M, Yang X, Wang S, Pi R, Rapposelli S. Nature-based molecules combined with rivastigmine: a symbiotic approach for the synthesis of new agents against Alzheimer's disease. Eur J Med Chem. 2017;141:232–9.

31. Iida A, Usui T, Zar Kalai F, Han J, Isoda H, Nagumo Y. Protective effects of Nitraria retusa extract and its constituent isorhamnetin against amyloid binduced cytotoxicity and amyloid b aggregation. Biosci Biotechnol Biochem. 2015;79:1548–51.

32. Fernandez-Bachiller MI, Perez C, Monjas L, Rademann J, Rodriguez-Franco MI. New tacrine-4-oxo-4H-chromene hybrids as multifunctional agents for the treatment of Alzheimer's disease, with cholinergic, antioxidant, and β-amyloid-reducing properties. J Med Chem. 2012;55:1303–17.

33. Moini H, Packer L, Saris NEL. Antioxidant and prooxidant activities of alpha-lipoic acid and dihydrolipoic acid. Toxicol Appl Pharmacol. 2002;182:84–90.

34. Holmquist L, Stuchbury G, Berbaum K, Muscat S, Young S, Hager K, Engel J, Münch G. Lipoic acid as a novel treatment for Alzheimer's disease and related dementias. Pharmacol Ther. 2007;113:154–64.

35. Maczurek A, Hager K, Kenklies M, Sharman M, Martins R, Engel J, Carlson DA, Münch G. Lipoic acid as an anti-inflammatory and neuroprotective treatment for Alzheimer's disease. Ad Drug Deliv Rev. 2008;60:1463–70.

36. Quinn JF, Bussiere JR, Hammond RS, Montine TJ, Henson E, Jones RE, Stackman RW Jr. Chronic dietary alpha-lipoic acid reduces deficits in hippocampal memory of aged Tg2576 mice. Neurobiol Aging. 2007;28(2):213–25.

37. Rosini M, Andrisano V, Bartolini M, Bolognesi ML, Hrelia P, Minarini A, Tarozzi A, Melchiorre C. Rational approach to discover multipotent anti-Alzheimer drugs. J Med Chem. 2005;48:360–3.

38. Sanga Z, Lia Y, Qiang X, Xiao G, Liu Q, Tan Z, Deng Y. Multifunctional scutellarin–rivastigmine hybrids with cholinergic, antioxidant, biometal chelating and neuroprotective properties for the treatment of Alzheimer's disease. Bioorg Med Chem. 2015;23:668–80.

39. Airoldi C, La Ferla B, D'Orazio G, Ciaramelli C. Palmioli A flavonoids in the treatment of Alzheimer's and other neurodegenerative diseases. Curr Med Chem. 2018;25:3228–46.

40. Jalili-Baleh L, Babaei E, Abdpour S, Bukhari SNA, Foroumadi A, Ramazani A, Sharifzadeh M, Abdollahi M, Khoobi M. A review on flavonoid-based scaffolds as multi-target-directed ligands (MTDLs) for Alzheimer's disease. Eur J Med Chem. 2018;152:570–89.

41. Melagraki G, Afantitis A, Igglessi-Markopoulou O, Detsi A, Koufaki M, Kontogiorgis C, Hadjipavlou-Litina DJ. Synthesis and evaluation of the antioxidant and anti-inflammatory activity of novel coumarin-3-aminoamides and their alpha-lipoic acid adducts. Eur J Med Chem. 2009;44:3020–6.

42. Hager K, Marahrens A, Kenklies M, Riederer P, Munch G. R-Lipoic acid as a new treatment option for Alzheimer type dementia. Arch Gerontol Geriatr. 2001;32:275–82.

43. Sang Z, Wang K, Shi J, Liu W, Cheng X, Zhu G, Wang Y, Zhao Y, Qiao Z, Wu A, Tan Z. The development of advanced structural framework as multi-target-directed ligands for the treatment of Alzheimer's disease. Eur J Med Chem. 2020;192:112180.

44. Bolognesi ML, Rosini M, Andrisano V, Bartolini M, Minarini A, Tumiatti V, Melchiorre C. MTDL design strategy in the context of Alzheimer's disease: from lipocrine to memoquin and beyond. Curr Pharm Des. 2009;15:601–13.

45. Agalave SG, Maujan SR, Pore VS. Click chemistry: 1,2,3-Triazoles as pharmacophores. Chem Asian J. 2011;6:2696–718.

46. Xu M, Peng Y, Zhu L, Wang S, Ji J, Rakesh KP. Triazole derivatives as inhibitors of Alzheimer's disease: current developments and structure-activity relationships. Eur J Med Chem. 2019;180:656–72.

47. Rastegari A, Nadri H, Mahdavi M, Moradi A, Mirfazli SS, Edraki N, Moghadam FH, Larijani B, Akbarzadeh T, Saeedi M. Design, synthesis and anti-Alzheimer's activity of novel 1,2,3-triazole-chromenone carboxamide derivatives. Bioorg Chem. 2019;83:391–401.

48. Naik MM, Tilve SG. Pyrrolidine and iodine catalyzed domino aldol-Michael-dehydrogenative synthesis of flavones. Tetrahedron Lett. 2014;55:3340–3.

49. Sagrera G, Bertucci A, Vazquez A, Seoane G. Synthesis and antifungal activities of natural and synthetic bioflavonoids. Bioorg Med Chem. 2011;19:3060–73.

50. Jaen JC, Wise LD, Heffner TG, Pugsley TA, Meltzer LT. Dopamine auto receptor agonists as potential antipsychotics. 2. (Aminoalkoxy)-4H-1-benzopyran-4-ones. J Med Chem. 1991;34:248–56.

51. Luo W, Su YB, Hong C, Tian RG, Su LP, Wang YQ, Li Y, Yue JJ, Wang CJ. Design, synthesis and evaluation of novel 4-dimethylamine flavonoid derivatives as potential multifunctional anti-Alzheimer agents. Bioorg Med Chem. 2013;21:7275–82.

52. Wu T, Zhang Q, Hu J, Zhang G, Liu S. Composite silica nanospheres covalently anchored with gold nanoparticles at the outer periphery of thermoresponsive polymer brushes. J Mater Chem. 2012;22:5155–63.

53. Garin D, Oukhatar F, Mahon AB, Try AC, Dubois-Dauphin M, Laferla FM, Demeunynck M, Sallanon MM, Chierici S. Proflavine derivatives as fluorescent imaging agents of amyloid deposits. Bioorg Med Chem Lett. 2011;21:2203–6.

54. Zsolt D, Juhász A, Gálfi M, Soós K, Papp R, Zádori D, Penke B. Method for measuring neurotoxicity of aggregating polypeptides with the MTT assay on differentiated neuroblastoma. Cells Brain Res Bull. 2003;62:223–9.

55. Ellman GL, Courtney KD, Andres V, Featherstone RM. A new and rapid colorimetric determination of acetylcholinesterase activity. Biochem Pharmacol. 1961;7:88–95.

56. Levine H. Thioflavine T interaction with synthetic Alzheimer's disease beta-amyloid peptide: detection of amyloid aggregation in solution. Protein Sci. 1993;20:404–10.

57. Baeeri M, Momtaz S, Navaei-Nigjeh M, Niaz K, Rahimifard M, GhasemiNiri SF, Sanadgol N, Hodjat M, Sharifzadeh M, Abdollahi M. Molecular evidence on the protective effect of ellagic acid on phosaloneinduced senescence in rat embryonic fibroblast cells. Food Chem Toxicol. 2017;100:8–23.

58. Benzie IFF, Strain JJ. Ferric reducing/antioxidant power assay: direct measure of total antioxidant activity of biological fluids and modified version for simultaneous measurement of total antioxidant power and ascorbic acid concentration. Methods Enzymol. 1999;299:15–27.

59. Pazik A, Skwierawska A. Synthesis and spectroscopic properties of new bis-tetrazoles. J Incl Phenom Macrocycl Chem. 2013;77:83–94.

60. Trott O, Olson AJ. AutoDock Vina: improving the speed and accuracy of docking with a new scoring function, efficient optimization and multithreading. J Comput Chem. 2010;31:455–61.

61. Dassault Systèmes BIOVIA. Discovery studio modeling, release, 4. San Diego: Dassault Systemes; 2015.